

1 The sugarless grape trait characterized by single berry phenotyping

2

3 **Antoine Bigard^{1,2}, Charles Romieu^{2,3}, Hernán Ojeda¹, Laurent Torregrosa^{1,4*}**

4

5 ¹UE INRAE de Pech Rouge, 11430, Gruissan, France.

6 ²AGAP, University of Montpellier, CIRAD, INRAE, Institut Agro, 34060 Montpellier Cedex, France.

7 ³GENOVIGNE, IFV, INRAE, Institut Agro, 2, place P. Viala, 34060 Montpellier Cedex, France

8 ⁴LEPSE, University of Montpellier, CIRAD, INRAE, Institut Agro, 34060 Montpellier Cedex, France.

9

10

11 ***Corresponding author:** laurent.torregrosa@supagro.fr

12

13 **Abstract**

14

15 For grape production, an important driver for the selection of varieties better adapted to
16 climate fluctuations, especially warming, is the balance between fruit sugars and acidity. Since
17 the past decades, temperature during ripening has constantly raised causing excessive sugars
18 concentrations and insufficient acidity of the wine grapes in warmest regions. There is thus an
19 increasing interest in breeding new cultivars, able to ripen at lower sugar concentration while
20 preserving fruit acidity. However, the phenotyping of berry composition challenges both
21 methodological and conceptual issues. Indeed, most authors predetermine either average
22 harvest date, ripening duration, thermal time or even hexoses concentration threshold itself,
23 to compare accessions at an hopefully similar ripe stage. Here, we have phenotyped the fruit
24 development and composition of 6 genotypes, including 3 new disease-tolerant varieties
25 known to produce wines with low alcoholic contents. The study was performed at single berry
26 level from the end of green growth stage to the arrest of phloem unloading, when water and
27 solute contents reach a maximum per berry. The results confirmed that sugarless genotypes
28 achieve fruit ripening with 20-30% less hexoses than classical varieties, Grenache N and Merlot
29 N, without impacting berry growth, total acidity or cations accumulation. Sugarless genotypes
30 displayed a higher malic acid/tartaric acid balance than other genotypes with similar
31 sucrose/H⁺ exchanges at the onset of ripening. Data suggest that sugarless phenotype results
32 from a specific plasticity in the relationship between growth and the turgor imposed by
33 organic acid accumulation and sugar loading. This opens interesting perspectives to
34 understand the mechanism of grapevine berry growth and to breed varieties better coping
35 with climate warming.

36

37 **Key words:** Fleshy fruit, fruit development, ripening, sugars, acidity, climate warming

38 **Introduction**

39 With an hexose concentration (glucose + fructose, [Hex]) higher than 1.1 mol.l⁻¹ at ripe stage,
40 grape is one of the richest fleshy fruits in sugars. [Hex] is accepted to depend on the GxExM
41 interaction (Suter et al., 2021) and until recently, cultivars adaptation to local conditions was
42 essentially reasoned according to the thermal time needed to reach specific vegetative and
43 reproductive phenological stages, as budburst, flowering or fruit veraison (Parker et al., 2020).
44 The selection of grapevine varieties is mainly driven by the balance between sugars and acidity
45 (Torregrosa et al., 2017; Ollat et al., 2018; Duchêne et al., 2020). In cold climates, early ripening
46 varieties are preferred to secure the accumulation of sugars and secondary metabolites before
47 autumn. Conversely, in warm regions, late ripening varieties shifting fruit ripening to cooler
48 days preserve organic acids (Rienth et al., 2016), anthocyanidin (Zhang et al., 2015) and aroma
49 compounds (Alessandrini et al., 2018; Asproudi et al., 2016; Gutiérrez-Gamboa et al., 2018).
50 But in practice a range of enological processes are implemented to correct sugars and/or acidity
51 of the must, demonstrating that the supposed adaptation of the varieties based on thermal time
52 phenology is oversimplified. Since the past decades, temperature during the period of grapevine
53 fruit ripening has constantly increased, which may lead to excessive sugars and insufficient
54 acidity in hot vine growing areas, such as mediterranean regions (Santillan et al., 2019, Bécart
55 et al., 2022). Especially, with the strength and the rate of ongoing climate changes, it is critical
56 to better objectify the development and the metabolism of the fruits to characterize their
57 adaptation potential (Bigard et al., 2018 and 2020). There is thus increased interest in breeding
58 new cultivars, able to ripen at lower sugar concentration while preserving fruit acidity.

59 Actually, warming doesn't simply accelerate the whole ripening process, which would be easily
60 solved by harvesting earlier but it decorrelates different aspects of ripening, accelerating malic
61 acid breakdown (Rienth et al., 2016, Sweetmann et al., 2014) while inhibiting the accumulation
62 of secondary metabolites such as anthocyanins, hence the decision to shift the date of harvest
63 to higher [Hex] (Arrizabalaga et al., 2018). Moreover, comparing cultivars at the same
64 developmental stage (the so-called ripe stage) raises both methodological and conceptual issues.
65 In most comparative studies, authors predetermine an average harvest date, ripening duration,
66 thermal time or even [Hex] threshold to compare accessions at an hopefully similar ripe stage,
67 in contradiction with the recognized impact of GxE on these variables (Liu et al., 2007; Dai et
68 al., 2011; Duchêne et al., 2012). To circumvent this inconsistency and lack of consensus, the
69 moment at which berry phloem unloading stops was recently proposed as a relevant definition
70 of ripe stage both on the physiological and transcriptomic point of views (Bigard et al., 2018

71 and 2020; Shahood et al., 2015 and 2020; Savoi et al., 2021). This key transition which marks
72 the arrest of the most intensive fruit biochemical pathways is associated with the transcriptional
73 extinction of many genes encoding, amongst other, sugar transporters, aquaporins and cell wall-
74 related enzymes (Savoi et al., 2021). Unfortunately, this developmental stage can't be directly
75 inferred from [Hex] kinetics, which continue to evolve after the completion of sugar storage (or
76 accumulation) due to subsequent berry shriveling. Thus, additional information on berry growth
77 is required to address the net rates of sugar accumulation and malic acid breakdown in berries,
78 together with their respective timings. Very recently, single berry phenotyping approaches
79 improved our understanding of berry growth and metabolism during ripening, avoiding the
80 biases due to berry asynchronicity (Shahood et al., 2020; Savoi et al., 2021). According to this
81 new paradigm, this study aims to decipher the genetic differences existing for [Hex] and fruit
82 acidity in a set of genotypes encompassing traditional varieties and new hybrids exhibiting low
83 [Hex] at harvest (Escudier et al., 2017; Ojeda et al., 2017).

84

85 **Materials and method**

86 **Plant Material and sampling method** - Experiments were performed outdoors at the INRAE
87 Pech Rouge experimental unit (Gruissan, France, 43.14'/3.14''W) under a semi-arid
88 Mediterranean climate in 2017 (temperature, rainfall and evapotranspiration data described
89 in Alem et al., 2021). Experimental plots were managed through drip irrigation keeping the
90 predawn leaf water potential (Ψ_{PD}) higher than -0.5 MPa (Giorgi & Lionello, 2008) to
91 correspond to a moderate water stress. The set of the genotypes encompassed 3 traditional
92 varieties Grenache N, Merlot N, and Morrastel N (<https://plantgrape.plantnet-project.org/fr/>)
93 and 3 new disease-resistant varieties deriving from 4 (3197-81B, 3197-373N) or 5 (3184-1-9N)
94 backcrosses of *Muscadinia rotundifolia* with *V. vinifera* varieties (Bouquet al., 1980). These 3
95 last genotypes are known to display a reduced [Hex] at harvest allowing the production of
96 wines at low ethanol levels, called VDQA, "**Vins De Qualité à teneur modérée en Alcool**" (Ojeda
97 et al. 2017). In the rest of the manuscript, the names G5, G7 and G14 will be respectively used
98 for 3197-81B, 3197-373N and 3184-1-9N. From 2 weeks before the first signs of berry
99 softening to 2 weeks later and during the rest of the ripening period over 1 week after fruit
100 shriveling, respectively 60 and 30 berries were weekly and randomly collected. Whole berries
101 were sampled between 9 and 11 AM by cutting the fruit peduncle just below the calyx,
102 maintained in a plastic bag in a cool place and analysed in the same day.

103 **Berry firmness and composition** - Firmness was monitored with a digital penetrometer called
104 Pénélaup™ (Abbal et al., 1992; Robin et al., 1997) as described in Shahood et al. (2020).
105 Immediately after firmness measurement, berries were immersed in 4 times their weight in
106 0.25N HCl. Seeds were immediately removed and samples incubated 48h. Samples were
107 vigorously shaken and a first 100 μL aliquot was 11 times diluted with $8.3 \cdot 10^{-3}$ N acetic acid
108 (internal control) + $16.4 \cdot 10^{-3}$ N sulphuric acid and centrifuged 5 min' at 18,500 g at 20°C,
109 supernatants were injected for HPLC to quantitate glucose, fructose, malic and tartaric acids
110 through a Biorad aminex-HPX87H column also described in Shahood et al. (2020). A second
111 100 μL aliquot was diluted 10 times in water and then 3 min centrifuged at 12000 rpm (20°C).
112 Ten μL clear supernatant was then injected in the HPLC through a Waters® IC-Pak Cation M/D
113 3.9x150 mm column with same parameters used in Bigard et al. (2020) in order to obtain
114 Potassium ($[\text{K}^+]$), Magnesium ($[\text{Mg}^{2+}]$) and Calcium ($[\text{Ca}^{2+}]$) concentrations. Titratable acidity
115 (TA) was calculated as the sum of malic and tartaric acids minus K^+ in $\text{mEq}\cdot\text{L}^{-1}$.

116 **Data normalisation and presentations** - R® software (version 4.1.2) was used to build
117 graphical representations and to analyse the data (R Core Team, 2017). Main packages used
118 for this study were “ggplot2” (Version 3.3.5), “car” (Version 3.0-12) and “rcompanion”
119 (Version 2.4.6).

120

121 **Results and discussion**

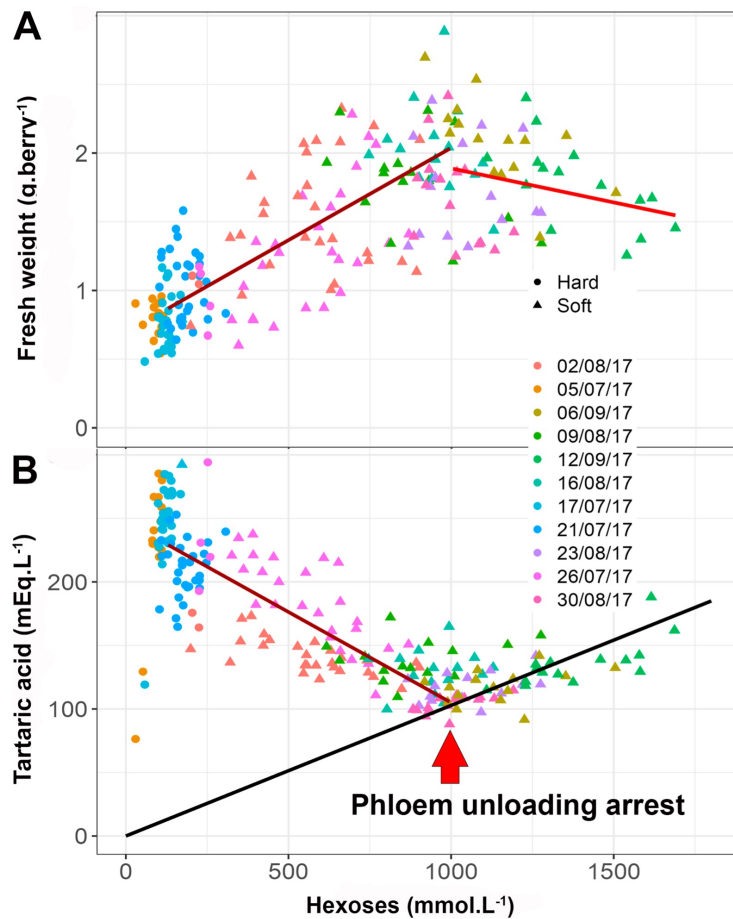
122 The grapevine displays small fruits clustered in grapes presenting a huge internal asynchrony
123 (Gouthu et al., 2014; Doumouya et al., 2014; Bigard et al., 2019; Shahood et al., 2020), as
124 illustrated in the next figures. Extrapolating single fruit metabolic traits from the averages
125 values observed on the population of berries led to biased kinetic interpretations and chimeric
126 metabolic concepts. In the grapevine where the berry is the only truly relevant physiological
127 unit, the most accurate method would be to non-destructively characterize each single fruit
128 kinetics (Castellarin et al., 2015; Savoi et al., 2021), which is only possible for morphological
129 attributes (fruit color and volume) and firmness. Regarding solute accumulation, hypodermal
130 sampling led to excessively elevated fluxes possibly resulting from injuring the berries, so its
131 validity was questioned (Coombe, 1992). Destructive sampling of density sorted berries or
132 large sets of individual fruits is then required to get accurate physiological insights on
133 grapevine fruit development (Rolle et al., 2011; Bigard et al., 2019; Shahood et al., 2020). Here,
134 we phenotyped the ripening of 3 new sugarless genotypes (G5, G7 and G14) and 3 traditional

135 varieties (Grenache N, Merlot N, Morrastel N) though the destructive chemical analysis of
136 thousands of single berries as in Shahood et al. (2020). Since it was not possible to measure
137 each individual flowering or softening dates, data are interpreted as a function of berry sugar
138 concentration, a proxy for internal time of fruit ripening (Rienth et al., 2016).

139 **Berry development and sugar accumulation**

140 **Figure 1** shows the evolution of berry weight and tartaric acid concentration during ripening
141 of Morrastel N, representative of the panel of varieties described in this study. Observed
142 trends are typical of *V. vinifera* genotypes with a nearly doubling berry volume and a twofold
143 dilution of tartaric acid during ripening. As described in Rienth et al. (2016) and in Bigard et al.
144 (2020), the dilution of tartaric acid appears to be a relevant indicator of berry relative growth
145 as its quantity doesn't evolve during and after ripening (Ruffner, 1982; Lang & Thorpe, 1989;
146 Terrier & Romieu, 2001; Rienth et al., 2014; Rösti et al., 2018; Burbidge et al., 2021). When
147 the uploading of sugars and water in the berries stops (Coombe & McCarthy, 2000; Conde et
148 al., 2007; Savoi et al., 2021), hexoses and tartaric acids just continue to concentrate due to
149 evaporation. This results in a linear regression passing through the origin as in **figure 1B**.
150 Tartaric acid concentration was obviously less heterogeneous than fresh berry weight facilitating
151 the identification of the max berry volume stage. With this method we could determine the
152 berry [Hex] at the maximum fruit volume for each variety, i.e. : 920 mmol.L⁻¹ for G5, 900
153 mmol.L⁻¹ for G7, 800 mmol.L⁻¹ for G14, 1125 mmol.L⁻¹ for Grenache N, 1125mmol.L⁻¹ for
154 Merlot N and 1000 mmol.L⁻¹ for Morrastel N. We used the 10 closest berries for each genotype
155 and both stages (end of green growth and max berry volume) to perform statistics as recorded
156 in **Table 1**. For the end of the green growth period, the 10 berries showing the highest malic
157 acid concentration were selected.

158



159

160 **Fig. 1** - Evolution of fresh weight (A) and tartaric acid concentration (B) of single berries of Morrastel during
161 ripening.

162

163 Despite genotypic differences in berry weight at green stage (**Fig. 2A**), the 6 genotypes
164 displayed the classical fruit expansion kinetics during ripening (Coombe, 1976). The relative
165 volume increment (i.e. $V_{ripe}/V_{veraison}$) was obtained using all combinations possible
166 between green and ripe selected berries and ranged from 1.8 ± 0.5 to 3.1 ± 0.7 , for Merlot
167 N and G5 respectively. Statistical analyses revealed that G5 had the highest berry growth
168 during ripening followed by G7 and Morrastel N, then G14 and Grenache N with Merlot N has
169 the least.

Genotype	Stage	FW (g.berry ⁻¹)		Text. (g.mm ⁻¹)		Hex. (mmol.L ⁻¹)		TA (meq.L ⁻¹)		MA (meq.L ⁻¹)		K (mmol.L ⁻¹)		Mg (mmol.L ⁻¹)		Ca (mmol.L ⁻¹)		Acidity (meq.L ⁻¹)	
		Mean	SD	Mean	SD	Mean	SD	Mean	SD	Mean	SD	Mean	SD	Mean	SD	Mean	SD	Mean	SD
G14	Green	1.3	0.4 ab	1993	428 ab	66	11 a	172	16 a	447	10 a	43	6 b	1.9	0.6 a	4.9	2.7 na	576	23 ab
G5		0.9	0.1 cd	1911	331 ab	73	15 ab	209	33 abc	547	25 b	44	8 b	1.6	1.0 a	4.5	2.2 na	712	54 c
G7		1.3	0.2 a	1683	605 ab	110	55 bcd	194	38 ab	552	30 b	42	5 b	2.8	1.1 ab	5.3	1.8 na	705	62 c
Grenache		1.1	0.3 abc	1861	446 ab	99	13 cd	219	32 bc	375	27 c	31	5 a	2.7	0.9 ab	4.6	0.7 na	562	38 a
Merlot		0.9	0.2 bcd	2088	431 b	78	17 abc	254	34 c	430	17 ac	55	5 c	3.7	1.0 b	5.4	1.6 na	629	37 bd
Morrastel		0.7	0.2 d	1490	356 a	122	14 d	248	17 c	451	11 a	45	6 b	2.9	0.6 b	4.4	1.0 na	655	16 cd
Test & Post-Hoc		Kruskal-Wallis & Dunn		Anova & Tukey		Kruskal-Wallis & Dunn		Kruskal-Wallis & Dunn		Kruskal-Wallis & Dunn		Kruskal-Wallis & Dunn		Anova & Tukey		Kruskal-Wallis & Dunn		Kruskal-Wallis & Dunn	
Genotype effect		4 10 ⁻⁵ ***		4.6 10 ⁻² *		1.6 10 ⁻⁵ ***		2 10 ⁻⁵ ***		9 10 ⁻¹⁰ ***		1 10 ⁻⁹ ***		7 10 ⁻⁵ ***		6.1 10 ⁻¹		1 10 ⁻⁸ ***	
G14	Ripe	2.5	0.3 b	163	79 na	809	33 a	80	8 ab	57	26 ab	56	6 b	2.0	0.4 a	1.9	0.5 a	80	25 a
G5		2.5	0.4 bc	152	41 na	918	13 b	75	10 a	72	30 ab	57	4 b	1.8	0.4 a	2.6	0.7 ab	90	36 a
G7		3.1	0.7 c	196	59 na	905	17 ab	98	19 bc	87	27 b	57	4 b	2.9	0.3 b	2.2	0.6 a	128	39 a
Grenache		2.2	0.5 ab	184	33 na	1130	23 c	105	12 cd	59	31 ab	47	8 a	2.7	0.5 b	2.8	0.8 ab	116	37 a
Merlot		1.6	0.3 a	217	89 na	1123	9 cd	126	18 e	42	19 a	64	6 b	3.7	0.6 c	3.7	0.8 b	104	36 a
Morrastel		1.8	0.4 a	154	43 na	997	9 bd	121	22 de	59	27 ab	64	8 b	2.9	0.7 b	3.0	1.9 ab	116	47 a
Test & Post-Hoc		Anova & Tukey		Anova		Kruskal-Wallis & Dunn		Anova & Tukey		Anova & Tukey		Anova & Tukey		Anova & Tukey		Kruskal-Wallis & Dunn		Anova & Tukey	
Genotype effect		2.61 10 ⁻⁸ ***		1.26 10 ⁻¹		1.5 10 ⁻¹⁰ ***		4 10 ⁻¹⁰ ***		1.3 10 ⁻² *		5 10 ⁻⁷ ***		2 10 ⁻¹¹ ***		5 10 ⁻⁴ ***		5 10 ⁻² *	

170

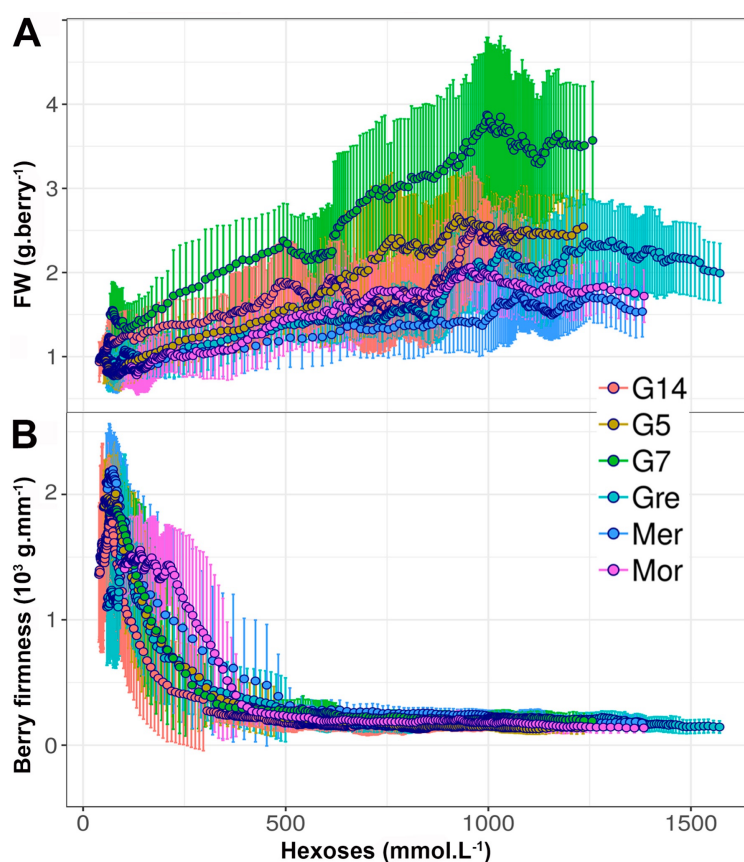
171 **Table 1** - Berry weight, firmness and composition of the 6 studied genotypes at the end of green growth phase
 172 and at physiological ripe stage. FW (Fresh weight), Text. (Texture), Hex (Hexoses), TA (Tartaric acid), MA (Malic
 173 acid). Statistical significance: * (p<0.01), ** (p<0.001), *** (P<0.0001), na (p>0.01).

174

175 Whatever the genotype, we observed a considerable heterogeneity in berry size at a similar
 176 [Hex], as previously reported (Gouthu et al. 2014; Vondras et al., 2016; Bigard et al. 2019;
 177 Shahood et al., 2020). Both the maximum volume of the berries and [Hex] at this stage varied
 178 according to the variety (**Fig. 2A**). [Hex] increased during ripening, from values around 100
 179 mmol.L⁻¹ at the end of the green growth phase to 0.8 to 1.1 mol.L⁻¹ at physiological ripe stage
 180 (**Table 1**). During berry ripening, with ca 0.5 M each, glucose and fructose became the major
 181 osmoticums as reported before in *V. vinifera* (Hawker et al., 1976; Liu et al., 2006; Shiraishi et
 182 al., 2010). [Hex] observed in this study at phloem arrest for the Merlot N and Grenache N are
 183 lower than the usual concentration threshold of 1.2 to 1.5 mol.L⁻¹ [Hex] at which the industry
 184 considers the berries as technologically ripe. Kliewer (1967) reported a range from 1 mol.L⁻¹
 185 to 1.5 mol.L⁻¹ [Hex] as the technical ripe grape for usual *V. vinifera* varieties. This apparent
 186 discrepancy is due to the very common practice to push grapes towards over-ripeness to get
 187 more redfull, aromatic wines and concentrated wines (Antalick et al., 2021). In the absence of
 188 supplementary physiological landmarks, the use of [Hex] for comparative studies is very
 189 hazardous, as this parameter steadily increases after phloem unloading arrest because of fruit
 190 shriveling (Friend et al., 2009; Shahood et al., 2020; **Fig. 2A**).

191 Sucrose unloading in berries of all genotypes dramatically increased at softening, or relaxation
 192 of turgor pressure (**Fig. S1**). All genotypes displayed a glucose/fructose higher than 2.2 before
 193 fruit softening, then the ratio progressively converged to 1 as reported in other *V. vinifera*

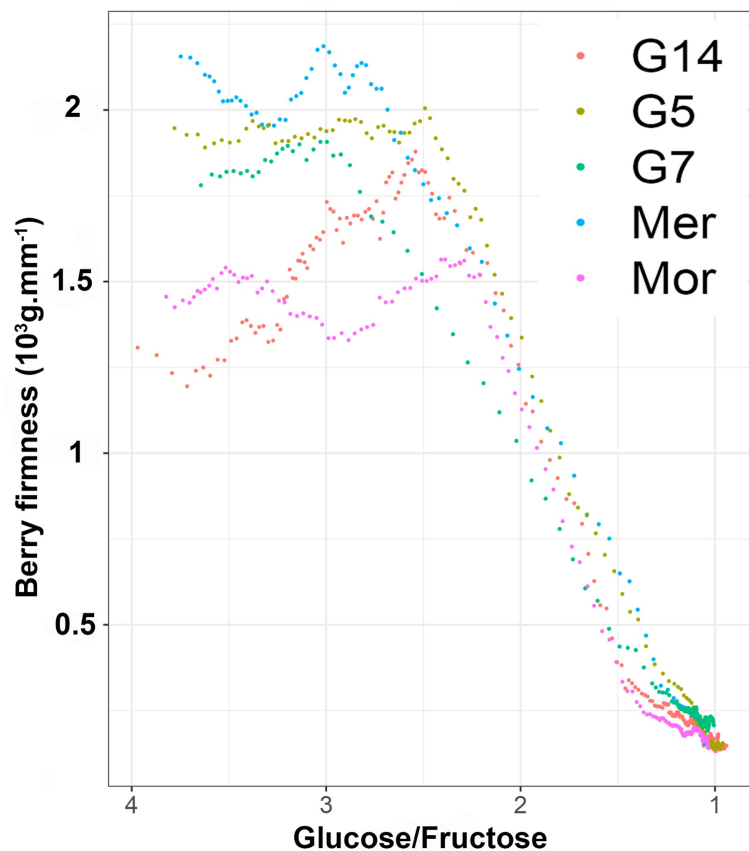
194 varieties (Varandas et al., 2004). No specific metabolic trends could be observed in the G
195 genotypes. It is known that berry glucose/fructose balance which depends on grapevine
196 organs and developmental stage can be used as a metabolic indicator of fruit ripening (Kliwer
197 et al., 1966). During green growth, the preferential use of fructose is obvious, leading to
198 elevated G/F ratio. At softening, the import of sucrose dramatically accelerates, exceeding
199 metabolic needs, insofar as malic acid replaces sugar as a respiratory substrate. Consequently,
200 the G/F ratio rapidly tends to 1 (Amerine and Thoukis, 1958; Liang et al., 2011; Houel et al.,
201 2015).
202



203
204 **Fig. 2** - Evolution of the berry fresh mass (A) and firmness (B) during the fruit ripening of 6 grapevine varieties.
205

206 Within a range of extreme varieties and offsprings Bigard et al. (2018) showed that [Hex] can
207 vary from 750 to 1350mmol.L⁻¹ when solute unloading stops just before berry shriveling. Here,
208 considering phloem arrest as the physiological ripe stage, G genotypes displayed [Hex] levels
209 between 0.8 and 0.9 mol.L⁻¹, Morrastel N was at 1 mol.L⁻¹, Merlot N and Grenache N showed
210 the highest [Hex] (> 1.1 mol.L⁻¹). These data agree with previous results obtained at the whole
211 berry population levels with similar genotypes (Ojeda et al., 2017; Bigard et al., 2019).
212 Interestingly, the final quantity of sugar per fruit unit in sugarless genotypes is of the same

213 magnitude as classical varieties, i.e : 2.8 +/- 0.3 mM (G7), 2.5 +/- 0.6 mM (G5), 2.3 +/- 0.4 mM
214 (G5), 2.0 +/- 0.3 mM (G14), 1.8 +/- 0.3 mM (Merlot) and 1.8 +/- 0.4 mM (Morrastel) per berry.
215 Before softening, berry firmness showed some differences in berries at the end of the green
216 growth phase with the Morrastel N and the Merlot N respectively showing the least and the
217 most firm fruits (**Table 1**). From the green growth phase, mechanical properties of the berries
218 evolved in the same way for all genotypes (**Fig. 2B**). Berries soften rapidly at the beginning of
219 ripening to reach a low level of firmness before 500 mmol.L⁻¹ of [Hex], i.e. more or less mid
220 ripening. Then, with a slow and continuous decrease of the firmness up to physiological ripe
221 stage and over-ripening, no firmness differences could be observed between sugarless
222 genotypes and traditional cultivars (**Table 1, Fig. S1**). Therefore, although firmness is widely
223 accepted as a sensitive and early indicator of the onset of ripening (Coombe et al. 1992; Abbal
224 et al., 1992; Castellarin et al., 2015; Shahood et al., 2020; Bigard et al., 2020), this parameter
225 can't be used to tag the transition at phloem unloading arrest. Consequently, the only way to
226 non destructively determine the shift from fruit expansion to shriveling remains the
227 monitoring of berry growth. As discussed below, this can be done indirectly, using Tartrate
228 concentration



229
230
231

Fig. S1 - Evolution of the berry firmness depending on glucose/fructose ratio during the fruit ripening.

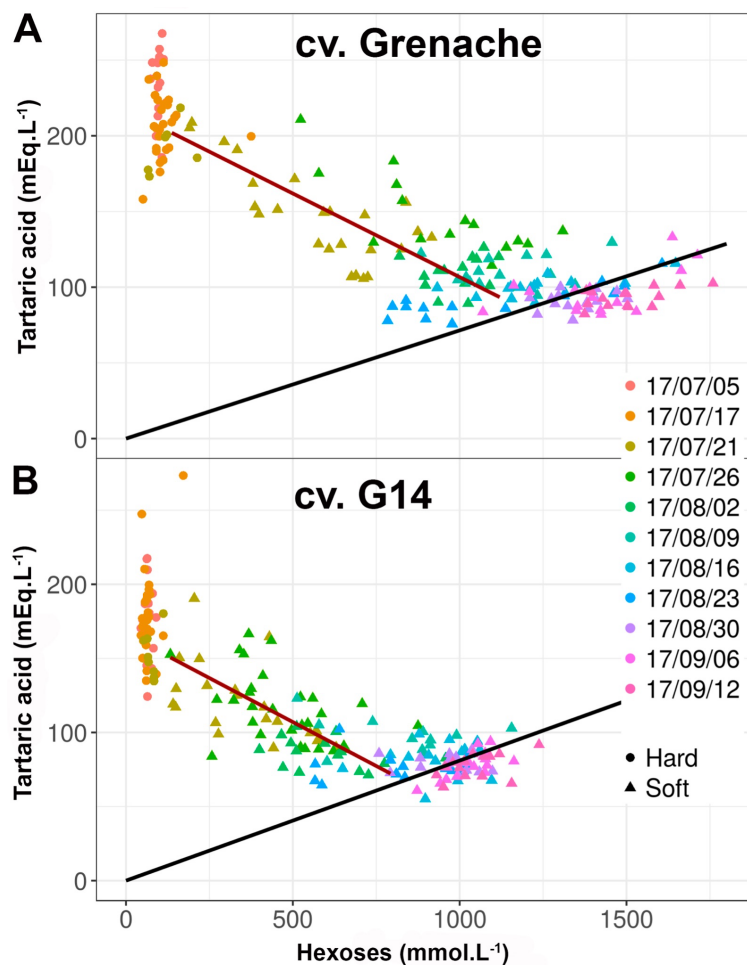
232 Evolution of the main determinants of fruit acidity

233 **Tartaric acid** - During ripening, tartaric concentration depended on the variety and the stage
234 of berry development (**Table 1**). At the onset of ripening, tartaric acid concentration was 25%
235 lower (150 vs 200 mEq.L⁻¹) in all G genotypes. Tartaric acid dilution (**Fig. S2**) proceeded at
236 negligible rate before 220 mmol.L⁻¹ (G5, G14) to 300 mmol.L⁻¹ [Hex] (Grenache N) and then
237 accelerated confirming the delay between berry softening and growth resumption (Castellarin
238 et al., 2015; Shahood et al., 2020 and other literature cited in this paper).

239 The change in tartaric acid from the starting to the end of ripening (**Fig. 3**), is consistent with
240 a first two to three fold dilution, followed by concentration due to shriveling, leading to a
241 linear increase in sugar and tartaric acid passing the origin. At the arrest of phloem unloading,
242 the concentration of tartaric acid reached a minimum ranging from 75 +/- 10 mEq.L⁻¹ (G5) to
243 126 +/- 18 mEq.L⁻¹ (Merlot N). Grenache N displayed a 104 +/- 12 mEq.L⁻¹ concentration in
244 tartaric acid at the ripe stage.

245

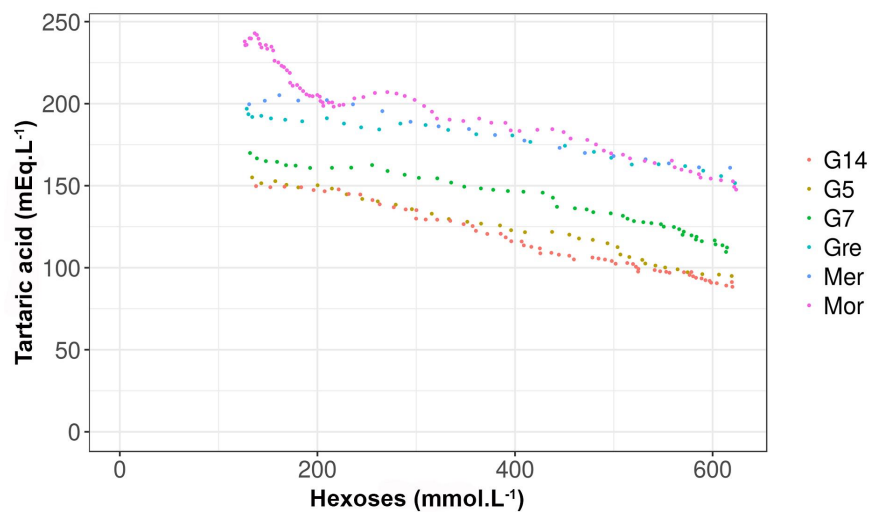
246



247

248 **Fig. 3** - Evolution of the tartaric acid concentration during berry ripening of Grenache (A) and G14 (B). Lines
249 corresponding to linear fitting during and after phloem unloading.
250

251



252

253 **Fig. S2** - Evolution of the tartaric acid concentration at the early stages ([Hex] from 125 and 625 mmol.L⁻¹) of fruit
254 ripening of 6 grapevine varieties.
255

256

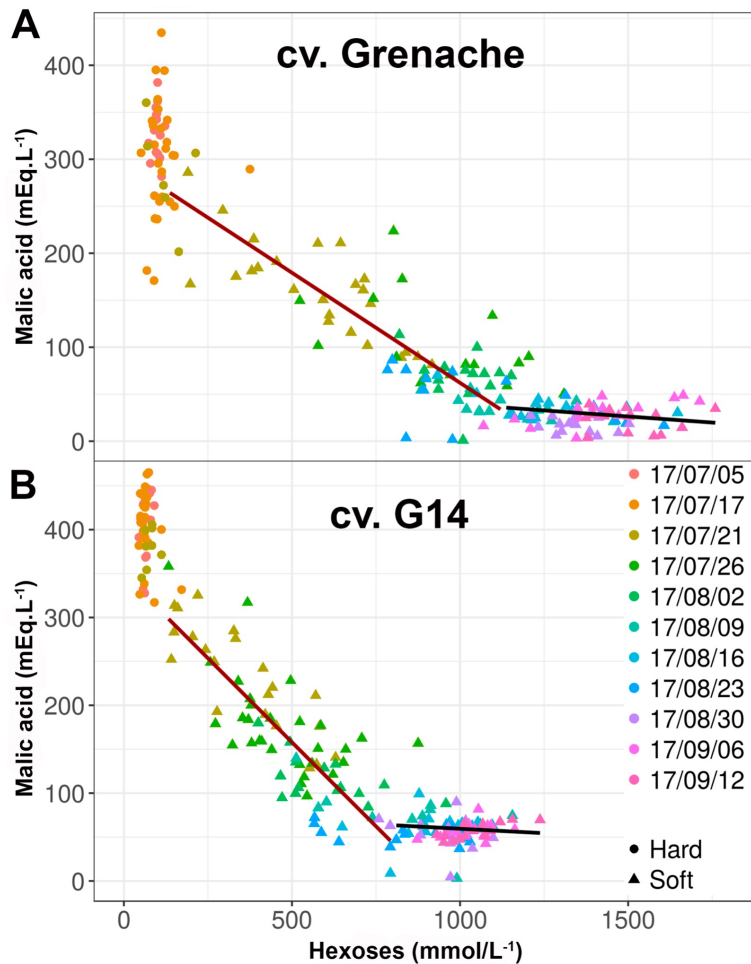
257

258 Tartaric acid is the first organic acid to be accumulated during young berry development and
259 remains one of the main acids in ripe fruits of *Vitis vinifera* (Amerine et al., 1965; Kliewer,
260 1966). In this study performed through single berry analysis, tartaric acid ranged from 170-
261 250 mEq.L⁻¹ at the beginning of ripening to decrease to 70-120 mEq.L⁻¹ at phloem stop as
262 previously observed (Bigard et al., 2019). Statistical analyses showed that, at the onset of
263 ripening, sugarless genotypes already display a lower tartaric acid concentration than
264 traditional cultivars. This trend is amplified at maximum volume stage due to the highest
265 expansion and resulting dilution (**Table 1**). Morrastel N, also called Graciano in Spain, is a
266 traditional cultivar producing wines rich in polyphenols with moderate ethanol levels (Ramos
267 and Martinez de Toda, 2021). We confirm here, through this study performed at single berry
268 level, that Morrastel N can produce ripe fruit at lower [Hex], i.e. below 1 mol.L⁻¹, in
269 comparison to other traditional varieties.

269 **Malic acid** - Malic acid concentration peaked at 370-550 mEq.L⁻¹ at the very end of green
270 growth period and then decreased to less than 90 mEq.L⁻¹ at maximum berry volume whatever
271 the genotype (**Table 1**). At the onset of ripening, conversely to tartaric acid, malic acid
272 concentration was higher in sugarless genotypes than in traditional varieties. At the arrest of
273 phloem unloading, the concentrations in malic acid ranged from 42 +/- 20 mEq.L⁻¹ (Grenache
274 N) to 87 +/- 26 mEq.L⁻¹ (G7), with no obvious genotypic effects. After phloem arrest, conversely

275 to tartaric acid, malic acid concentration stayed stable or even slightly decreased (**Fig. 4**), as
276 observed in previous studies performed at berry population levels (Ojeda et al., 2017; Bigard
277 et al., 2019).

278



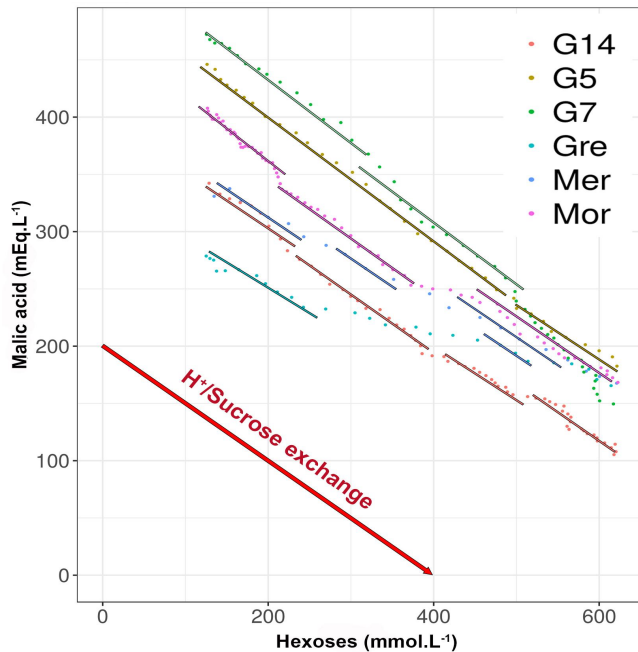
279

280 **Fig. 4** - Evolution of the malic acid concentration during berry ripening of Grenache (A) and G14 (B). Lines
281 corresponding to linear fitting during and after phloem unloading.

282

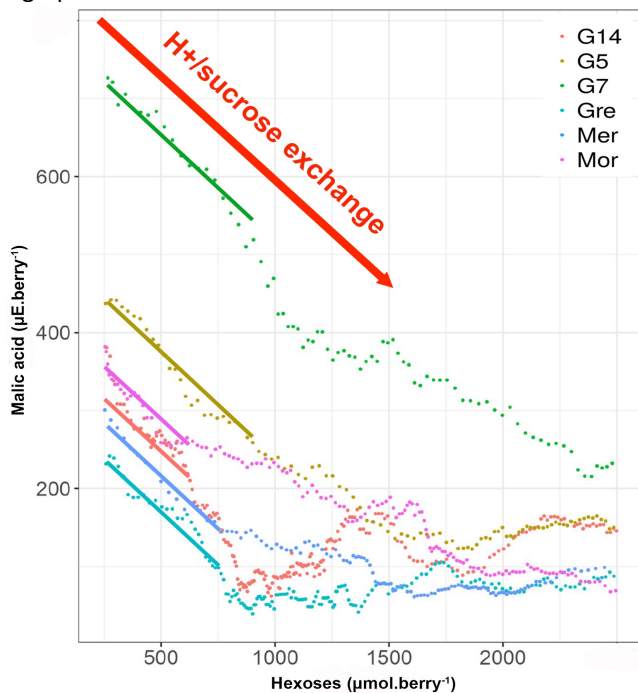
283 Malic acid respiration provides a major fraction of the energy during early ripening (Famiani
284 et al., 2014; Shahood, 2017), hence a faster decrease in concentration than if only dependent
285 on dilution due to berry growth. Here, despite different starting points (**Table 1, Fig. S3**), the
286 decrease of malic acid during the first phase of ripening (i.e. from 250 to 800 $\mu\text{mol}\cdot\text{berry}^{-1}$
287 [Hex]), was characterized by an initial slope of -1 mEq per 2 hexoses, noticeably similar in the
288 6 genotypes (**Fig. S3**). During early ripening, the initial changes in the respective amounts of
289 malic acid and sugar per fruit (concentration x volume; **Fig. 5**) are fully consistent with the
290 activation of a sucrose/H⁺ exchanger on the tonoplast of all *V. vinifera* cultivars investigated,
291 including sugarless genotypes, which generalizes our quantitative data on Syrah and Pinot

292 (Shahood et al., 2020). In single berries, the corresponding genes are strongly expressed until
293 phloem arrest (Savoi et al., 2021). At the beginning of ripening, the sucrose/H⁺ exchange is
294 electro-neutralized by the release of vacuolar malate, as detected here, while more and more
295 H⁺ must be redirected to the vacuole as malic acid vanishes, as illustrated by the progressive
296 activation of vacuolar ATPase and PPIase (Terrier et al., 2001).



297

298 **Fig. S3** - Repeatability of the malic acid/sugar exchange during early berry ripening (125-625 mmol.L⁻¹ [Hex]) of
299 6 grapevine varieties.



300

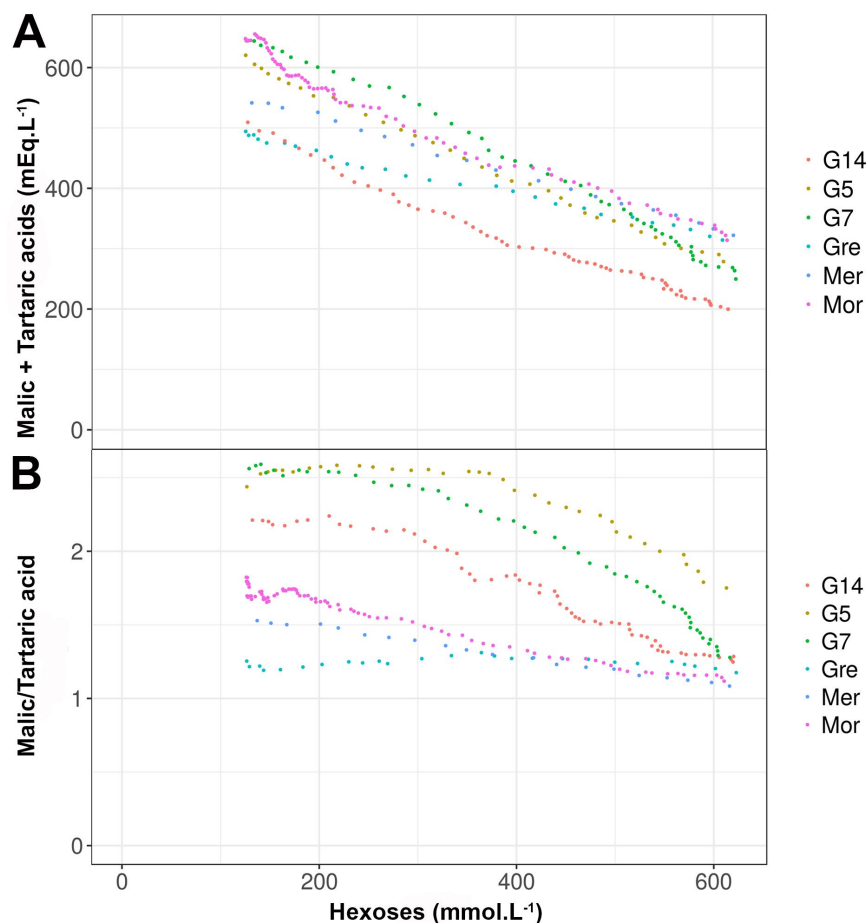
301

302 **Fig. 5** - Repeatability of the malic acid/sugar exchange expressed in quantity per fruit during berry ripening of 6
303 grapevine varieties.

304

305 When the cumulative evolution of tartaric + malic acids was monitored during early ripening
306 (**Fig. S4 A**), no specific behaviors could be observed in the sugarless genotypes in comparison
307 to the other varieties. Considering that, according to their concentrations, sugars and organic
308 acids are the main contributors to the osmotic potential of the berry (Matthews et al., 1987),
309 present results totally exclude that the reduction in sugar concentration may be compensated
310 by a greater accumulation of organic acids in the sugarless genotypes. As mentioned before,
311 sugarless genotypes displayed lower tartaric and higher malic acid than traditional controls
312 and consequently an higher malic acid/tartaric acid ratio (**Fig. S4 B**).

313



314

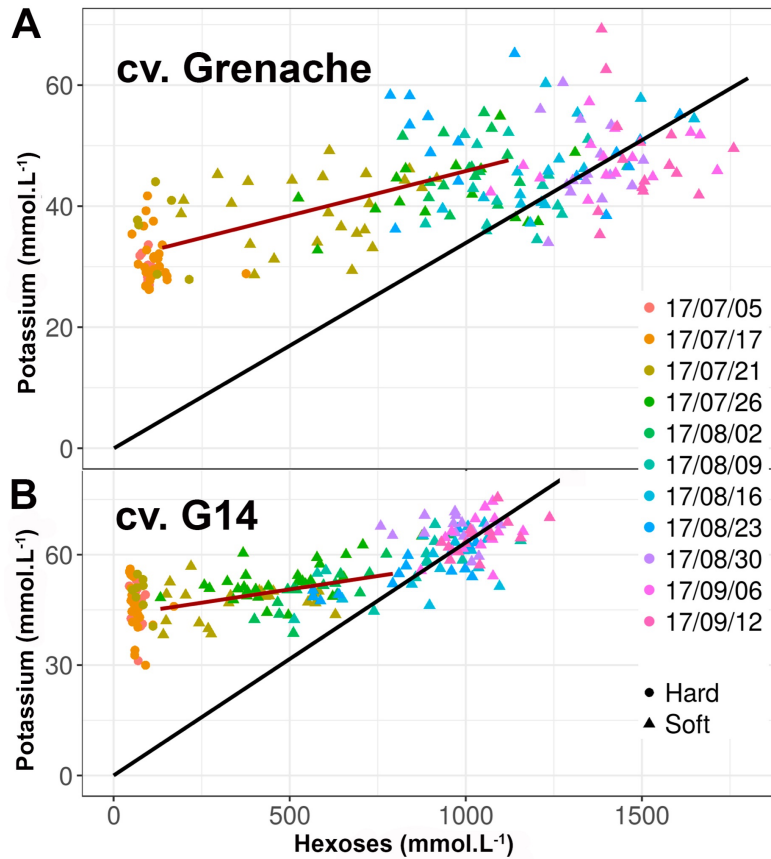
315 **Fig. S4** - Evolution of the sum of malic and tartaric acid concentration (A) and malate/tartrate (B) during early
316 berry ripening (125-625 mmol.L⁻¹ [Hex]) of 6 grapevine varieties.

317

318 **Potassium** - K⁺, the main cation in the grapevine fruit, is accumulated during both phases of
319 growth (Cuellar et al., 2013). Here, concentrations before ripening ranged from 31 ± 5 mEq.L⁻¹
320 for Grenache N to 55 ± 5 mEq.L⁻¹ for the Merlot N (**Table 1**). During ripening, [K⁺] increased
321 moderately during ripening (**Fig. S5**) with increments ranging from 16% (Merlot N) to 50%
322 (Grenache N) both genotypes displaying the lower and the higher levels of [K⁺] at the ripe

323 stage, respectively 47 ± 8 mEq.L⁻¹ for Grenache N and 64 ± 6 mEq.L⁻¹ for Merlot N. After the
324 period of phloem loading arrest, as for tartaric acid, [K⁺] steadily increased in link to water
325 loss associated with shriveling (**Fig. 6**).

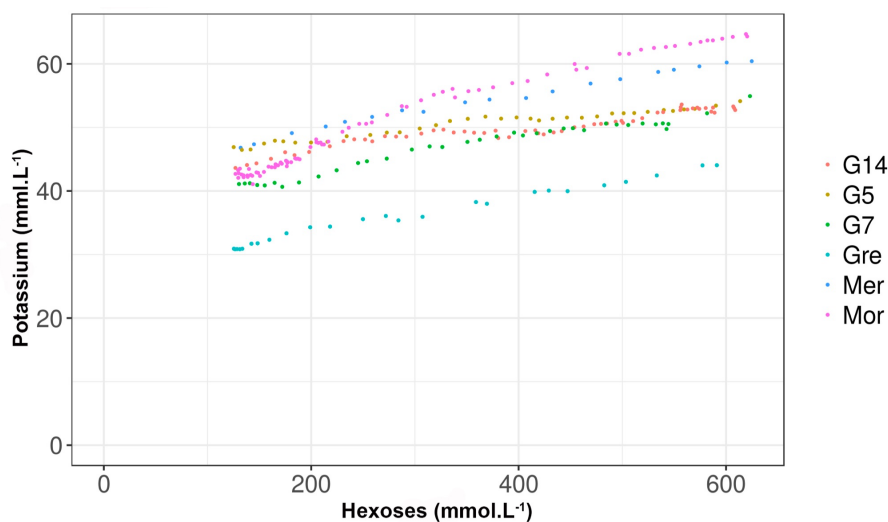
326



327

328 **Fig. 6** - Evolution of the potassium concentration during berry ripening of Grenache (A) and G14 (B). Lines
329 corresponding to linear fitting during and after phloem unloading.

330



331

332 **Fig. S5** - Evolution of the potassium concentration during early ripening (125-625 mmol.L⁻¹ [Hex]) of 6 grapevine
333 varieties.

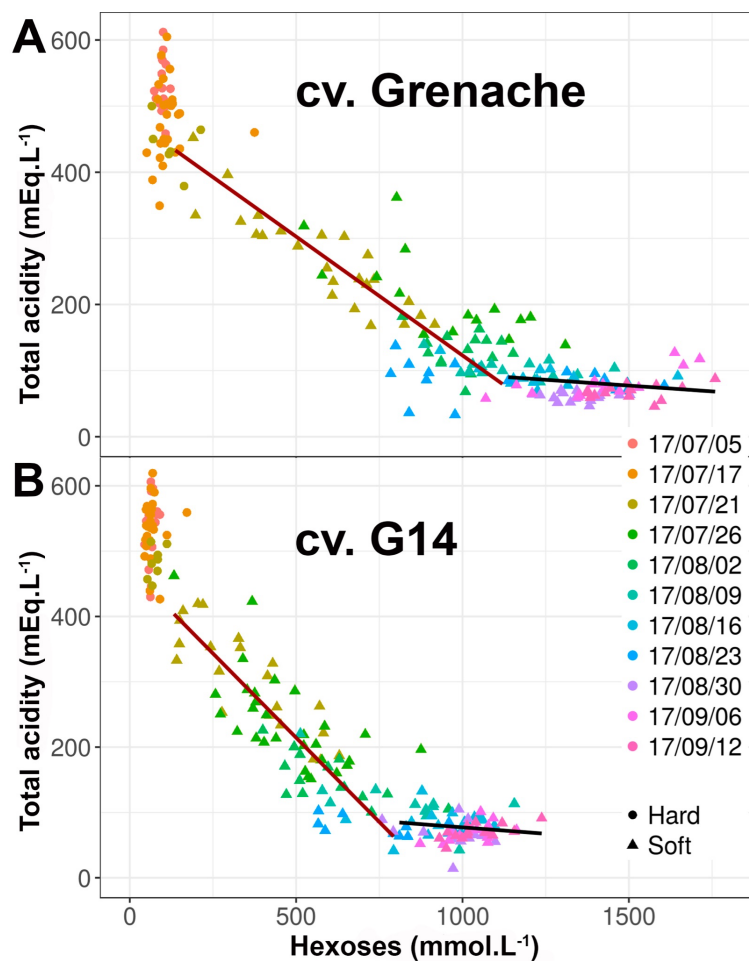
334

335 After main organic compounds, K^+ is the fourth contributor to berry osmotic potential, also
336 neutralizing a fraction of organic acids (Storey, 1987; Rogiers et al., 2017). During early stages
337 of development, low sugar accumulators (Morrastel N included) had a higher $[K^+]$ than high
338 accumulators (**Table 1**). This element being mainly accumulated in the skin may play a role in
339 the difference in elasticity from G genotypes. At the end of phloem unloading the average $[K^+]$
340 is around 50 mmol.L^{-1} in the 6 genotypes, suggesting a strong homeostasis for this element.
341 During the phloem unloading period from veraison to max berry volume, as observed at
342 population level with other genotypes (Bigard et al., 2020), K^+ concentration increased 20-40
343 times less than hexoses (**Fig. 5, Fig. S5, Table 1**).

344 This obviously contradicts the so-called "massive" K^+ import in the ripening berry (Villette et
345 al., 2020). As recently discussed by Savoi et al. (2021), the belief that K^+ transport would
346 compensate for an intrinsic deficiency in the energisation of sugar imports is not supported
347 by experimental data. In this respect, the simultaneous and parallel increases in $[Hex]$ and
348 $[K^+]$ observed after the arrest of phloem unloading, isn't indicative of a co-transport
349 mechanism, but only results from a net water loss and berry shriveling. Despite significant
350 progress in the understanding of the import of potassium in grapevine berries (Rogiers et al.,
351 2017; Villette et al., 2020; Savoi et al., 2021), the putative mechanistic links between potassium
352 and sugar imports still remain speculative.

353 **Evolution of the fruit acidity** - Green berries displayed a high acidity (**Fig. 7, Table 1**) ranging
354 from $560 \pm 40 \text{ mEq.L}^{-1}$ (Grenache N) to $710 \pm 50 \text{ mEq.L}^{-1}$ (G5). As the results of tartaric acid
355 dilution, malic acid respiration and dilution, and slight K^+ accumulation, acidity was reduced
356 to $80 \pm 25 \text{ mEq.L}^{-1}$ (G14) to 130 ± 40 (G7) at the ripe stage with no statistical differences
357 between genotypes. Noticeably, the total acidity tended to increase very late the ripe stage
358 for all genotypes, ca $1250 \text{ mmol.L}^{-1} [Hex]$ in Grenache N, and $1000 \text{ mmol.L}^{-1} [Hex]$ in G14.

359



360

361 **Fig. 7** - Evolution of the juice total acidity during berry ripening of Grenache (A) and G14 (B). Lines corresponding
362 to linear fitting during and after phloem unloading.

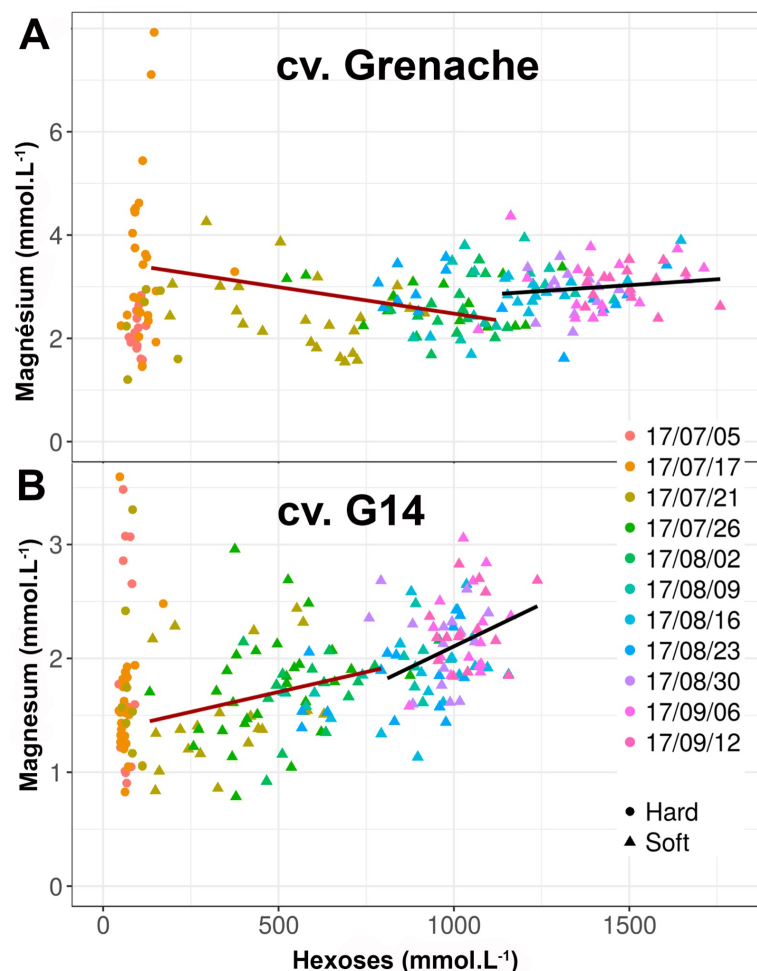
363

364 Acidity is a major challenge for wine quality (Champagnol, 1984; Sweetman et al., 2014; Ollat
365 et al., 2018). The effect of temperature on grape acidity is well documented (Kliwer and Lider,
366 1970; Butrose et al., 1971; Seguin et al., 2004; Rienth et al., 2016). By virtue of the
367 electroneutrality principle, titratable (or total) acidity represents the difference between acids
368 (mainly tartaric and malic in grapevine) and cations (mainly K⁺ in plants) . The reports of
369 Bigard et al. (2018; 2020), Duchène et al. (2020), that detailed the genetic diversity for anions
370 (i.e. organic acids) and cations and the consequence in grape acidity in a set of extreme *V.*
371 *vinifera* varieties and offsprings, here we analyzed the determinants of the acidity of 6
372 varieties, including 3 sugarless genotypes. As shown in previous sections, sugarless genotypes
373 tend to display a malic acid/tartaric acid ratio higher than the 3 traditional cultivars but with
374 similar sums of malic + tartaric acids and K⁺ levels. As the results, the sugarless genotypes
375 presented similar levels of acidity at the same physiological ripe stage than other varieties.

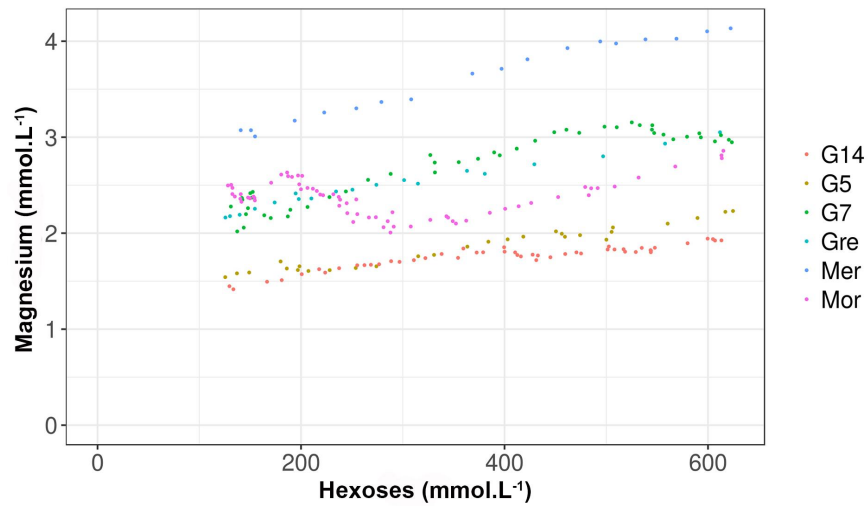
376 **3. Other cations (Mg²⁺, Ca²⁺)**

377

378 Magnesium (Mg^{2+}) was much less accumulated than K^+ in all genotypes. $[Mg^{2+}]$ displayed very
379 few changes during ripening (**Table 1, Fig. S6, Fig. S7**). At the arrest of phloem unloading,
380 $[Mg^{2+}]$ ranged from 1.6 +/- 1.0 (G5) to 3.7 +/- 1.0 (Merlot N) $mEq.L^{-1}$. Ranging from 4.5 +/- 2.2
381 (G5) to 5.4 +/- 1.6 (Merlot N) $mEq.L^{-1}$, Calcium (Ca^{2+}) was found more accumulated in the green
382 berries than Mg^{2+} (**Table 1**). Then during ripening, $[Ca^{2+}]$ tended to decrease (**Fig. S8 and S9**),
383 ending with concentrations of 1.9 +/- 0.5 (G14) to 3.7 +/- 0.8 (Merlot N) $mEq.L^{-1}$, a relative
384 decrease quite comparable to that of tartaric acid. Therefore, its total amount per berry
385 remains constant during ripening, as widely accepted in grapevine, and consistent with its
386 almost exclusive transport by xylem (Glad et al., 1992; Creasy et al., 1993). Both cations didn't
387 have a major impact on the wine quality and presented very few variations within the panel
388 of varieties.
389

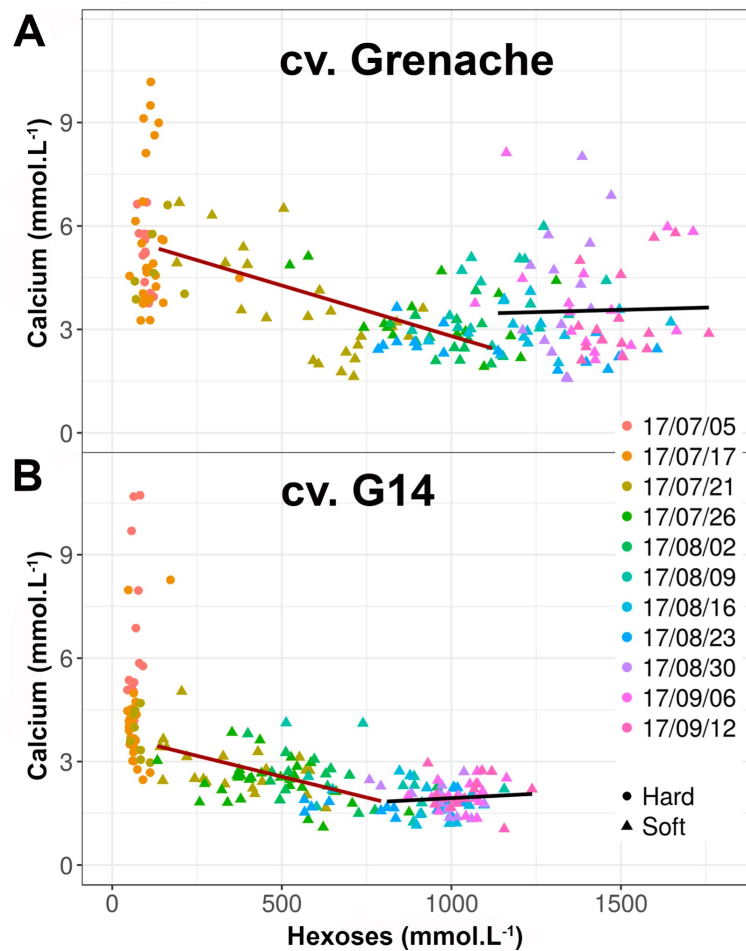


390
391 **Fig. S6** - Evolution of the magnesium concentration during berry ripening of Grenache (A) and G14 (B). Lines
392 corresponding to linear fitting during and after phloem unloading.
393



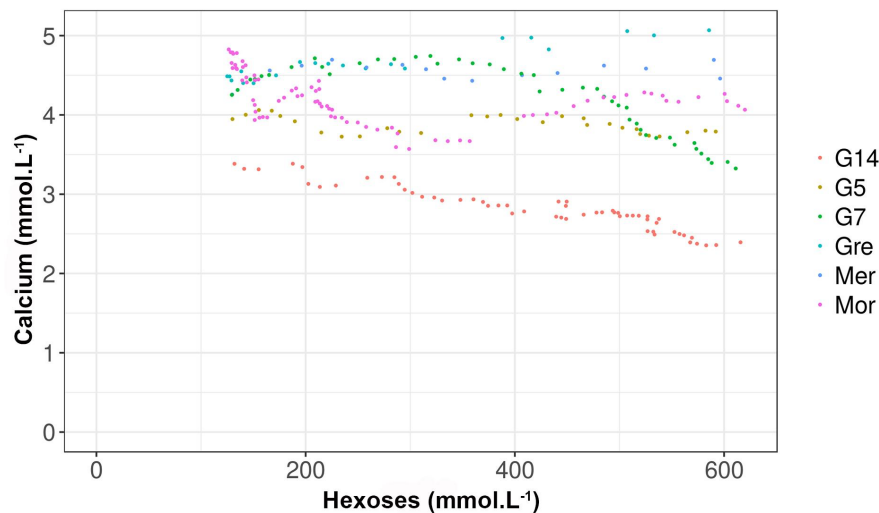
394
395
396
397
398

Fig. S7 - Evolution of the magnesium concentration during early ripening (125-625 mmol.L⁻¹ [Hex]) of 6 grapevine varieties.



399
400
401
402
403

Fig. S8 - Evolution of the calcium concentration during berry ripening of Grenache (A) and G14 (B). Lines corresponding to linear fitting during and after phloem unloading.



404
405
406

Fig. S9 - Evolution of the calcium concentration during early ripening ($125\text{-}625\text{ mmol.L}^{-1}$ [Hex]) of 6 grapevine varieties.

407
408

Conclusion

410

411 Getting fruits with reduced [Hex] while preserving their acidity represents an option to
412 mitigate the effect of climate warming on grapevine fruit quality (Torregrosa et al., 2017). This
413 objective can't be fully addressed by viticultural practices, e.g. harvesting before complete
414 sugar unloading or removing a fraction of the leaves to reduce C photoassimilation, without
415 impacting the quality of the wines (Bobeica et al., 2015; Antalick et al., 2021). Some diversity
416 can be found in *V. vinifera* varieties, or can be obtained by crossbreeding, for water, sugars
417 and the determinants of acidity of the grape (Bigard et al., 2018, 2020). In this study, using
418 advanced methods of berry phenotyping, we have characterized the fruit development and
419 ripening of a set of new disease-tolerant varieties producing low alcoholic wines (Escudier et
420 al., 2017). In previous studies, we have shown that combining single fruit phenotyping and
421 precise physiological landmarks significantly improve the understanding of berry development
422 features (Shahood et al., 2020; Savoi et al., 2021). Indeed, relations between the major solutes
423 are no longer biased upon averaging unsynchronized hence developmentally and
424 metabolically chimeric samples. To circumvent the imprecision of berry growth curves
425 resulting from the heterogeneity in berry size, tartaric acid dilution was used to detect the
426 timing of phloem unloading arrest. This study showed that the sugarless genotypes display a
427 [Hex] reduced by 20-30% when reaching ripe stage without impacting berry growth, organic
428 acid and cations accumulation levels. No major difference being found for fruit growth rates
429 and the quantity of sugars per berry in comparison to control varieties, this suggests the

430 sugarless phenotypes undergo a greater cellular expansion at similar osmotic or turgor
431 pressure. This property is not specific to genotypes deriving from *Muscadinia rotundifolia* and
432 table grape varieties, because Morrastel N also displayed a limited [Hex] in the ripe fruit (< 1
433 mol.L⁻¹). Moreover, similar behaviors can be found in other traditional varieties, such as
434 Aramon, Cornifesto and Mandilaria (Bigard et al., 2018) and Glera, a variety used for Prosecco
435 wine production (<https://plantgrape.plantnet-project.org/fr/cepage/Glera>). Taken together
436 our results show that adaptive traits to climate changes can be pyramided with QTLs of
437 tolerance to diseases. By crossing G5 and G14, we have generated microvine segregating
438 progenies (Torregrosa et al., 2019) to further characterize the physiology of this trait and
439 investigate the genetic determinism of water, sugar and organic accumulations (Savoi et al.,
440 2021).

441

442 **Acknowledgements** - Thanks to Eleoneora Maoddi, Yannick Sire and Philippe Abbal for their
443 contribution in the experiments.

444

445 **References**

446

- 447 Abbal, P., Boulet, J. C. & Moutounet, M. (1992). Utilisation de paramètres physiques pour la caractérisation de la
448 véraison des baies de raisin. J. Int. Sci. Vigne Vin, 26, 231-237.
- 449 Alem, H., Ojeda, H., Rigou, P., Schneider, R. & Torregrosa L. (2021). The reduction of plant sink/source does not
450 systematically improve the metabolic composition of the *Vitis vinifera* white fruit. Food Chem., 345,
451 128825. <https://doi.org/10.1016/j.foodchem.2020.128825>.
- 452 Alessandrini, M., Gaiotti, F., Belfiore, N., Matarese, F., D'Onofrio, C. & Tomasi D. (2018). Influence of vineyard
453 altitude on Glera grape ripening (*Vitis vinifera* L.): effects on aroma evolution and wine sensory profile. J
454 Sci Food Agric., 97, 2695-2705.
- 455 Amerine, M. A. & Thoukis, G. (1958). The glucose/fructose ratio of California grapes. *Vitis*, 1, 224-229.
- 456 Amerine, M. A., Roessler, E. B. & Ough, C. S. (1965). Acids and the acid taste. I. The effect of pH and titratable
457 acidity. Am. J. Enol. Vitic., 16, 29-37.
- 458 Antalick, G., Šuklje, K., Blackman, J. W., Schmidtke, L. M. & Deloire A. (2021). Performing sequential harvests
459 based on berry sugar accumulation (mg/berry) to obtain specific wine sensory profiles. *OenoOne*, 55, 131–
460 146. <https://doi.org/10.20870/oeno-one.2021.55.2.4527>.
- 461 Arrizabalaga, M., Morales, F., Oyarzun, M., Delrot, S., Gomès, E., Irigoyen, J. J., Hilbert, G. & Pascual I. (2018).
462 Tempranillo clones differ in the response of berry sugar and anthocyanin accumulation to elevated
463 temperature. *Plant Sci.*, 267, 74-83. doi: 10.1016/j.plantsci.2017.11.009.
- 464 Asproudi, A., Petrozziello, M., Cavalletto, S. & Guidoni S. (2016). Grape aroma precursors in cv. Nebbiolo is
465 affected by vine microclimate. *Food Chem.*, 211, 947-956.
- 466 Becard, V., Lacroix, R., Puech, C. & Inaki Garcia de Cortozar-Atauri (2022). Assessment of changes in Grenache
467 grapevine maturity in a Mediterranean context over the last half-century. *OenoOne*, 56.
468 <https://doi.org/10.20870/oeno-one.2022.56.1.4727>.
- 469 Bigard, A., Berhe, D. T., Maoddi, E., Sire, Y., Boursiquot, J. M., Ojeda, H., Péros, J. P., Doligez, A., Romieu, C. &
470 Torregrosa L. (2018). *Vitis vinifera* L. fruit diversity to breed varieties anticipating climate changes.
471 *Frontiers Plant Sci.*, doi: 10.3389/fpls.2018.00455.
- 472 Bigard, A., Romieu, C., Sire, Y., Veyret, M., Ojeda, H. & Torregrosa L. (2019). Grape ripening revisited through
473 berry density sorting. *OenoOne* 4, 719-724. DOI:10.20870/oeno-one.2019.53.4.2224.

- 474 Bigard, A., Romieu, C., Sire, Y. & Torregrosa L. (2020). *Vitis vinifera* L. diversity for cations and acidity is suitable
475 for breeding fruits coping with climate warming. *Frontiers Plant Sci.*, DOI: 10.3389/fpls.2020.01175.
- 476 Bobeica, N., Poni, S., Hilbert, G., Renaud, C., Gomès, E., Delrot, S. & Dai Z. (2015). Differential responses of sugar,
477 organic acids and anthocyanins to source-sink modulation in Cabernet Sauvignon and Sangiovese
478 grapevines. *Front. Plant Sci.*, 382. doi:10.3389/fpls.2015.00382.
- 479 Burbidge, C. A., Ford, C. M., Melino, V. J., Wong, D. C. J., Jia, Y., Jenkins, C. L. D., Soole, K. L., Castellarin, S. D.,
480 Darriet, P., Rienth, M., Bonghi, C., Walker, R. P., Famiani, F. & Sweetman C. (2021). Biosynthesis and
481 cellular functions of tartaric acid in grapevines. *Frontiers Plant Sci.*, 12. doi:10.3389/fpls.2021.643024.
- 482 Butrose, M. S., Hale, C. R. & Kliewer W. M. (1971). Effect of temperature on the composition of Cabernet-
483 Sauvignon berries. *Am. J. Enol. Vitic.*, 22, 71-75.
- 484 Castellarin, S. D., Gambetta, G. A., Wada H., Krasnow M. N., Cramer G. R., Peterlunger E., Shackel K. A. & Matthews
485 M. A. (2015). Characterization of major ripening events during softening in grape: turgor, sugar
486 accumulation, abscisic acid metabolism, colour development, and their relationship with growth. *J. Exp.*
487 *Bot.* 67, 709-722. doi: 10.1093/jxb/erv483.
- 488 Champagnol F. (1984). *Éléments de physiologie de la vigne et de viticulture générale*, ed. Dehan (Montpellier,
489 France: Dehan).
- 490 Conde C., Silva P., Fontes N., Dias A., Tavares R.M., Sousa M.J., Agasse A., Delrot S., Gerós H. (2007)
491 Biochemical Changes throughout Grape Berry Development and Fruit and Wine Quality. *Food 1*: 1-22.
- 492 Coombe, B. G. (1976). The development of fleshy fruits. *An. Rev. Plant Physiol.*, 27, 507-528.
- 493 Coombe, B. G. (1992). Research on development and ripening of the grape berry. *Am. J. Enol. Vitic.*, 43, 101-
494 110.
- 495 Coombe, B. G. & McCarthy, M.G. (2000). Dynamics of grape berry growth and physiology of ripening. *Aust. J.*
496 *Grape Wine Res.*, 6, 131-135. doi:10.1111/j.1755-0238.2000.tb00171.x.
- 497 Cuellar, T., Azeem, F., Andrianteranagna, M., Pascaud, F., Verdeil, J. L., Sentenac, H., Zimmermann, S. & Gaillard
498 I. (2013). Potassium transport in developing fleshy fruits: the grapevine inward K⁺ channel VvK1.2 is
499 activated by CIPK-CBL complexes and induced in ripening berry flesh cells. *Plant J.*, 73, 1006-1018. doi:
500 10.1111/tpj.12092.
- 501 Dai, Z. W., Ollat, N., Gomès, E., Decroocq, S., Tandonnet, J. P., Bordenave, L. et al. (2011). Ecophysiological,
502 genetic, and molecular causes of variation in grape berry weight and composition: a review. *Am. J. Enol.*
503 *Vitic.*, 62, 413-425. doi: 10.5344/ajev.2011.10116.
- 504 Doumouya, S., Lahaye, M., Maury, C. & Siret R. (2014) Physical and physiological heterogeneity within the grape
505 bunch: impact on mechanical properties during maturation. *Am. J. Vitic. Enol.*, 65, 170-178. doi:
506 10.5344/ajev.2014.13062.
- 507 Duchêne, E., Dumas, V., Jaegli, N. & Merdinoglu D. (2012). Deciphering the ability of different grapevine
508 genotypes to accumulate sugar in berries. *Aust. J. Grape Wine Res.*, 18, 319-328. doi: 10.1111/j.1755-
509 0238.2012.00194.x.
- 510 Duchêne, E., Dumas, V., Butterin, G., Jaegli, N., Rustenholtz, C., Chauveau, A., Berard, A., Le Paslier, M. C., Gaillard,
511 I. & Merdinoglu D. (2020). Genetic variations of acidity in grape berries are controlled by the interplay
512 between organic acids and potassium. *Theor. App. Genet.*, <https://doi.org/10.1007/s00122-019-03524-9>.
- 513 Escudier, H., Bigard, A., Ojeda, H., Samson, A., Caillé, S., Romieu, C. & Torregrosa L. (2017) De la vigne au vin : des
514 créations variétales adaptées au changement climatique et résistant aux maladies cryptogamiques 1/2 :
515 La résistance variétale. *Revue des Oenologues*, 44, 16-18.
- 516 Famiani, F., Farinelli, D., Palliotti, A., Moscatello, S., Battistelli, A. & Walker R. B. (2014). Is stored malate the
517 quantitatively most important substrate utilised by respiration and ethanolic fermentation in grape berry
518 pericarp during ripening? *Plant Physiol. Biochem.*, 76, 52-57. doi: 10.1016/j.plaphy.2013.12.017.
- 519 Friend, A.P., Trought M.C.T. & Creasy G. L. (2009). The influence of seed weight on the development and growth
520 of berries and live green ovaries in *Vitis vinifera* L. cvs. Pinot noir and Cabernet-Sauvignon. *Aust. J. Grape*
521 *Wine Res.*, 15, 166-174.
- 522 Gouthu, S., O'Neil, S. T., Di, Y., Ansarolia, M., Megraw, M. & Deluc L.G. (2014). A comparative study of ripening
523 among berries of the grape cluster reveals an altered transcriptional programme and enhanced ripening
524 rate in delayed berries. *J. Exp. Bot.*, 65, 5889-5902. doi: 10.1093/jxb/eru329.
- 525 Gutiérrez-Gamboa, G., Garde-Cerdán, T., Carrasco-Quiroz, M., Pérez-Álvarez, E.P., Martínez-Gil, A.M., Del Alamo-
526 Sanza, M. & Moreno-Simunovic Y. (2018). Volatile composition of Carignan noir wines from ungrafted and
527 grafted onto País (*Vitis vinifera* L.) grapevines from ten wine-growing sites in Maule Valley, Chile. *J Sci*
528 *Food Agric.*, 98, 4268-4278.
- 529 Hawker, J. S., Ruffner, H. P. & Walker R.R. (1976). The sucrose content of some Australian grapes. *Am. J. Enol.*
530 *Vitic.*, 27, 125-129.

- 531 Houel, C., Chatbanyong, R., Doligez, A. Rienth, M., Foria, S., Luchoire, N., Roux, C., Adivèze, A., Lopez, G., Farnos,
532 M., Pellegrino, A., This, P., Romieu, C. & Torregrosa L. (2015). Identification of stable QTLs for vegetative
533 and reproductive traits in the microvine (*Vitis vinifera* L.) using the 18K Infinium chip. BMC Plant Biol.,
534 15,205. DOI 10.1186/s12870-015-0588-0.
- 535 Kliewer, W. M. (1966). Sugars and Organic Acids of *Vitis vinifera*. Plant Physiol., 41, 923-931.
536 <http://www.jstor.org/stable/4260763>.
- 537 Kliewer, W. M. (1967). The glucose-fructose ratio of *Vitis vinifera* grapes. Am. J. Enol. Vitic., 18, 33-41. doi:
538 10.1016/j.aca.2011.11.043.
- 539 Kliewer, W. M. & Lider L.A. (1970). Effect of day temperature and light intensity on growth and composition of
540 *Vitis vinifera* L. fruits. J. Amer. Soc Hortic. Sci., 95, 766–769.
- 541 Lang, A. & Thorpe M. R. (1989). Xylem, phloem and transpiration flows in a grape: application of a technique for
542 measuring the volume of attached fruits to high resolution using Archimedes' principle. J. Exp. Bot., 40,
543 1069–1078. doi: 10.1093/jxb/40.10.1069.
- 544 Liang, Z., Sang, M., Fan, P., Wu, B., Wang, L., Duan, W. & Li S. (2011). Changes of polyphenols, sugars, and organic
545 acid in 5 *Vitis* genotypes during berry ripening. J. Food Sci., 76, 1231-1238.
- 546 Liu, H., Wu, B., Fan, P., Xu, H. & Li S. (2006). Sugar and acid concentrations in 98 grape cultivars analyzed by
547 principal component analysis. J. Sci. Food Agric., 86, 1526-1536. doi: 10.1002/jsfa.2541.
- 548 Liu, H., Wu, B., Fan, P., Xu, H. & Li S. (2007). Inheritance of sugars and acids in berries of grape (*Vitis vinifera* L.).
549 Euphytica, 153, 99-107. doi: 10.1007/s10681-006-9246-9.
- 550 Matthews, M. A., Cheng, G. & Weinbaum S. A. (1987). Changes in water potential and dermal extensibility during
551 grape berry development. J. Amer. Soc. Hort. Sci., 112, 314-319.
- 552 Ojeda, H., Bigard, A., Escudier J. L., Samson, A., Caillé, S., Romieu, C. & Torregrosa L. (2017). De la vigne au vin :
553 des créations variétales adaptées au changement climatique et résistant aux maladies cryptogamiques
554 2/2 : Approche viticole pour des vins de type VDQA. Revue des Œnologues, 44, 22-27.
- 555 Ollat, N., Marguerit, E., Lecourieux, F., Destrac-Irvine, A., Barrieu, F., Dai, Z. et al. (2018). Grapevine adaptation
556 to abiotic stresses. Acta Hort., 1248. doi: 10.17660/ActaHortic.2019.1248.68.
- 557 Parker, A. K., de Cortázar-Atauri, I. G., Gény, L., Spring, J. L., Destrac, A., Schultz H., et al. (2020). Temperature-
558 based grapevine sugar ripeness modeling for a wide range of *Vitis vinifera* L. cultivars. Agric. For.
559 Meteorol., 285, 107902. doi: 10.1016/j.agrformet.2020.107902.
- 560 Ramos, M. C. & Martínez de Toda F. (2021). Interannual and spatial variability of grape composition in the Rioja
561 DOC show better resilience of cv. Graciano than cv. Tempranillo under a warming scenario. OenoOne 55,
562 85-100. <https://doi.org/10.20870/oeno-one.2021.55.3.4695>.
- 563 R Core Team (2017). R: A Language and Environment for Statistical Computing. Vienna: R Foundation for
564 Statistical Computing.
- 565 Rienth, M., Torregrosa, L., Luchoire, N., Chatbanyong, R., Lecourieux, D., Kelly, M., et al. (2014). Day and night
566 heat stress trigger different transcriptomic responses in green and ripening grapevine (*Vitis vinifera*) fruit.
567 BMC Plant Biol., 14,108. doi: 10.1186/1471-2229-14-108.
- 568 Rienth, M., Torregrosa, L., Gauthier, S., Ardisson, M., Brillouet J. L. & Romieu C. (2016). Temperature
569 desynchronizes sugar and organic acid metabolism in ripening grapevine fruits and remodels its
570 transcriptome. BMC Plant Biol., 16, 164. DOI 10.1186/s12870-016-0850-0.
- 571 Robin, J. P., Abbal, P. & Salmon J.M. (1997) Firmness and grape berry maturation: definition of different
572 rheological parameters during the ripening. J. Int. Sci. Vigne Vin, 31, 127-138.
573 <https://doi.org/10.20870/oeno-one.1997.31.3.1083>.
- 574 Rogiers, S. Y., Coetzee, Z. A., Walker, R. R., Deloire, A. & Tyerman S.D. (2017). Potassium in the grape (*Vitis vinifera*
575 L.) berry: transport and function. Frontiers Plant Sci., 8, 1629. <https://doi.org/10.3389/fpls.2017.01629>.
- 576 Rolle, L., Giacosa, S., Gerbi, V., Bertolino, M. & Novello V. (2013). Varietal comparison of the chemical, physical,
577 and mechanical properties of five colored table grapes. Int. J. Food Prop., 16, 598-612.
578 <http://dx.doi.org/10.1080/10942912.2011.558231>.
- 579 Rösti, J., Schumann, M., Cleroux, M., Lorenzini, F., Zufferey, V., Rienth, M. (2018). Effect of drying on tartaric acid
580 and malic acid in Shiraz and Merlot berries. Aust. J. Grape Wine Res., 24, 421-429. doi:
581 10.1111/ajgw.12344.
- 582 Ruffner, H. P. (1982). Metabolism of tartaric and malic acids in *Vitis*: A review - Part A. Vitis, 21, 247–259. doi:
583 10.5073/VITIS.1982.21.247-259.
- 584 Santillán, D., Iglesias, A., La Jeunesse, I., Garrote, L. & Sotes V. (2019). Vineyards in transition: A global assessment
585 of the adaptation needs of grape producing regions under climate change. Science of The Total
586 Environment, 657, 839-852. <https://doi.org/10.1016/j.scitotenv.2018.12.079>.

- 587 Savoi, S., Torregrosa, L. & Romieu C. (2021). Transcripts repressed at the stop of phloem unloading highlight the
588 energy efficiency of sugar import in the ripening *V. vinifera* fruit. Hort. Res., 8, 193.
589 <https://doi.org/10.1038/s41438-021-00628-6>.
- 590 Seguin, B., Stevez, L., Herbin, C. & Rochard J. (2004). Changements climatiques et perspectives pour la viticulture:
591 conséquences potentielles d'une modification du climat. Revue des Oenologues, 111, 59-60.
- 592 Shahood, R., Rienth, M., Torregrosa, L. & Romieu C. (2015). Evolution of grapevine (*Vitis vinifera* L.) berry
593 heterogeneity during ripening. 19th International Meeting of Viticulture GIESCO. Vol. 2, pp. 564–567.
- 594 Shahood R. (2017). The berry within an asynchronous harvest: A new paradigm towards the quantitative
595 interpretation of sugar and acid fluxes as major osmoticums and respiratory substrates during bimodal
596 grape development. PhD of Montpellier SupAgro, <http://www.theses.fr/s206075>, 215 p.
- 597 Shahood, R., Torregrosa, L., Savoi, S. & Romieu C. (2020). Berry development hidden by its non-synchronous
598 population. OenoOne, 54, 1077-1092. <https://doi.org/10.20870/oeno-one.2020.54.4.3787>.
- 599 Shiraiishi, M., Fujishima, H. & Chijiwa H. (2010). Evaluation of table grape genetic resources for sugar, organic
600 acid, and amino acid composition of berries. Euphytica, 174, 1-13. doi: 10.1007/s10681-009-0084-4.
- 601 Storey ,R. (1987). Potassium localization in the grape berry pericarp by energy-dispersive x-ray microanalysis.
602 Am. J. Enol. Vitic., 38, 301-309.
- 603 Suter, B., Destrac-Irvine, A., Gowdy, M., Dai, Z. &van Leeuwen C. (2021) Adapting wine grape ripening to global
604 change requires a multi-trait approach. Front. Plant Sci., 12, 624867. doi: 10.3389/fpls.2021.624867.
- 605 Sweetman, C., Sadras, V. O., Hancock, R. D., Soole, K. L., Ford, C. M. (2014). Metabolic effects of elevated
606 temperature on organic acid degradation in ripening *Vitis vinifera* fruit. J. Exp. Bot., 65, 5975–5988. doi:
607 10.1093/jxb/eru343.
- 608 Terrier, N., Sauvage, F. X., Ageorges, A. & Romieu C. (2001). Changes in acidity and in proton transport at the
609 tonoplast of grape berries during development. Planta, 213, 20-28.
610 <http://www.jstor.org/stable/23386210>.
- 611 Torregrosa, L., Bigard, A., Doligez, A. Lecourieux, D. Rienth, M., Luchaire, N., Pieri, P. Chatbanyong, R., Shahood,
612 et al. (2017). Developmental, molecular and genetic studies on the grapevine response to temperature
613 open breeding strategies for adaptation to warming. OenoOne, 51, 155-165. DOI: 10.20870/oeno-
614 one.2016.0.0.1587.
- 615 Torregrosa, L., Rienth, M., Romieu, C. & Pellegrino A. (2019). The microvigne, a model for grapevine physiology
616 studies and genetics. OenoOne, 53. DOI: <https://doi.org/10.20870/oeno-one.2019.53.3.2409>.
- 617 Varandas, S., Teixeira, M. J., Marques, J. C., Aguilar, A., Alves, A., & Bastos M. (2004). Glucose and fructose levels
618 on grape skin: interference in *Lobesia botrana* behaviour. Analytica Chimica Acta, 513, 351-355.
619 ,doi:10.1016/j.aca.2003.11.086.
- 620 Villette, J., Cuélar, T., Verdeil, J. L., Delrot, S. & Gaillard I. (2020). Grapevine potassium nutrition and fruit quality
621 in the context of climate change. Front. Plant Sci., 11, 123. doi: 10.3389/fpls.2020.00123.
- 622 Vondras, A. M., Gouthu, S., Schmidt, J. A., Petersen, A. R. & Deluc, L. G. (2016). The contribution of flowering time
623 and seed content to uneven ripening initiation among fruits within *Vitis vinifera* L. cv. Pinot noir clusters.
624 Planta, 243, 1191-1202.
- 625 Zhang, C., Jia, H., Wu, W., Wang, X., Fang, J. & Wang C. (2015). Functional conservation analysis and expression
626 modes of grape anthocyanin synthesis genes responsive to low temperature stress. Gene, 574, 168-177.
627
628
629
630
631